Comparative Study of Maleated Polyolefins as Compatibilizers for Polyethylene/Wood Flour Composites

Sun-M. Lai,[1] Feng-C. Yeh,[2] Yeh Wang,[2] Hsun-C. Chan,[2] Hsiao-F. Shen[3]

[1] *Department of Chemical Engineering, Chinese Culture University, Taipei, Taiwan, 111 Republic of China*
[2] *Department of Chemical Engineering, Tunghai University, Taichung, Taiwan, 407 Republic of China*
[3] *R&D Department, Plastics Industry Development Center, Taichung, Taiwan, 407 Republic of China*

Received 9 July 2001; accepted 22 April 2002

ABSTRACT: The effects of various types of compatibilizers on the mechanical properties of high-density polyethylene/wood flour composites were investigated. Functionalized polyolefins, including maleated polyethylenes, polypropylene, and styrene–ethylene/butylene–styrene copolymer, were incorporated to reduce the interfacial tension between the polyethylene matrix and wood filler. Of these, maleated linear low-density and high-density polyethylenes gave higher tensile and impact strengths for the composites, presumably because of their better compatibility with the high-density polyethylene matrix. Similar but less enhanced improvements in the mechanical properties, depending on the compatibilizer loading, were seen for a maleated styrene–ethylene/butylene–styrene triblock copolymer, whereas maleated polypropylene only slightly improved the tensile modulus and tensile strength, which increased with increasing compatibilizer loadings. Scanning electron microscopy was used to reveal the interfacial region and confirm these findings. Dynamic mechanical thermal measurements showed the interaction between the filler and the matrix. Fourier transform infrared spectroscopy was used to assign the chemical fixation and the various chemical species involved on the surfaces of the fillers before and after surface treatment. © 2002 Wiley Periodicals, Inc. J Appl Polym Sci 87: 487–496, 2003

Key words: compatibilizer; maleated polyolefin; polyethylene/wood flour composite

INTRODUCTION

Polymer composites featuring both stiffness and strength have been of great commercial interest for a century now. Although inorganic fillers such as calcium carbonate, mica, fiberglass, talc, and clay have been widely used, composites containing organic fillers derived from renewable resources have aroused broad interest because of growing environmental concerns and the increasing costs of inorganic fillers. In particular, cellulose-based fillers, such as wood flour (WF) and cellulose fibers, have been used to yield composites with the additional advantages of low density relative to inorganic systems, biodegradability, and nonabrasiveness to processing equipment. Although opportunity exists for other sources of wood to be used as filler materials for thermoplastics, WF, being a commercially available resource derived from postindustrial scrap, is one of the most commonly used wood-derived fillers today.

WF-reinforced plastic composites have found applications in various areas, including automotive interior, household, ornament, building, and packaging uses. However, the use of cellulose-based materials as reinforcements or fillers for polyolefins has only recently gained acceptance. This is because the inclusion of cellulosic fillers in polyolefins usually gives rise to reduced toughness and poor stress-transfer efficiency that results from incompatibility between the polar and hydrophilic filler and the nonpolar and hydrophobic matrix. When polyolefins are used as thermoplastic matrices, there must be some form of interaction between the thermoplastic matrix and filler for useful composites to be realized.

The improvement in interfacial adhesion between cellulosic fillers and thermoplastics has been the focus of a large amount of research during the past 2 decades. Several comprehensive reviews have been published recently.[1–4] Cellulosic fillers can be modified by physical and chemical methods. Among various ways of chemical modification for polyolefin/WF composites,[5–11] the functionalized polyolefins are most often tested because of their efficiency and commercial availability.

Many producers are now selling functionalized polyolefins, including Epolene from Eastman Kodak, Polybond from Uniroyal, Fusabond from DuPont, Hercoprime from Himont, and Kraton from Shell. These products are made by the modification of olefinic polymers such as polypropylene (PP), polyethylene (PE), and ethylene/butylene–styrene triblock copolymer. They differ not only by the chemical nature

Correspondence to: Y. Wang (yehwang@mail.thu.edu.tw).

Journal of Applied Polymer Science, Vol. 87, 487–496 (2003)

of the polymer and by the degree of grafting but also by the molecular weight, that is, the chain length of the polymer backbone. In addition, the distribution of the grafted functional groups along the backbone may also be important. Maleated polypropylenes (PP-*g*-MAs) have long been known to increase adhesion between WF and polyolefin resins, resulting in improvements in the physical properties of WF/PP composites.[12–21] When a PE matrix is to be reinforced, PP-*g*-MA is not favored because of the incompatibility between PE and PP.[4,13] Therefore, the use of functionalized PEs or polymers with ethylene blocks is then a better choice.

Raj and Kokta[22] examined the effects of coupling agents on the tensile properties of high-density polyethylene (HDPE)/WF composites. They found that the addition of maleated polyethylene (PE-*g*-MA; Epolene C-18) gave better properties than stearic acid and other agents. Oksman and coworkers[23–25] also investigated the mechanical properties and morphology of PE/WF composites modified with a styrene–ethylene/butylene–styrene triblock copolymer grafted with maleic anhydride (SEBS-*g*-MA). They showed that the incorporation of a compatibilizer enhanced both the tensile strength and impact strength of the resulting composites. An electron microscopy study revealed improved adhesion between the filler and matrix. The observed effects were attributed to the interfacial bonding between maleic anhydride on styrene–ethylene/butylene–styrene (SEBS) and hydroxyl groups on the WF surfaces. Besides, physical interaction between the SEBS backbone and the polyolefin matrix was important for improving the interfacial adhesion between phases. Other composite systems with PE as the matrix also demonstrated the usefulness of functionalized ethylene-propylene-diene rubber (EPDM) and PE.[26,27]

Although considerable work has been carried out on the mechanical properties of polyolefin/WF or fiber composites, only a few studies have focused on the differences in modifications resulting from the structural characteristics of compatibilizers. Numerous variables, such as the WF mesh size, resin melt flow, and loading of the compatibilizers, are important in modifying filler surface. Nevertheless, two inherent properties of functionalized polyolefins significantly influencing their effectiveness as compatibilizers are (1) the chemical structure and molecular weight, which could affect miscibility and entanglement with the base resin, and (2) the degree of grafting, which determines the amount of functionality present in the agents.

In this study, various diagnostic methods were applied to evaluate the effectiveness of polyolefinic compatibilizing agents on the basis of the two major parameters mentioned previously. The compounding of PE and WF on a self-wiping, corotating twin-screw extruder has been proven effective.[28] Compatibilizers, mainly functionalized polyolefins, were incorporated to lower the interfacial tension between the PE matrix and wood filler. Mechanical properties, including the tensile strength and Izod impact strength, were investigated. The fracture surface was studied through scanning electron microscopy (SEM) to elucidate the interfacial region between the matrix and wood filler. Dynamic mechanical thermal analysis (DMTA) measurements provided information about the interface between the filler and matrix. Fourier transform infrared (FTIR) spectroscopy was used to assign the chemical fixation and various chemical species involved at the surfaces of the fillers before and after surface treatment.

EXPERIMENTAL

Materials

The materials used in this study were HDPE, WF, and four kinds of functionalized polyolefins: maleated linear low-density polyethylene (LLDPE-*g*-MA), maleated high-density polyethylene (HDPE-*g*-MA), SEBS-*g*-MA, and PP-*g*-MA. It was expected that the use of PE-*g*-MAs could enhance the interfacial compatibility between the wood filler and HDPE matrix. SEBS-*g*-MA was used because it was a well-known impact modifier. PP-*g*-MA was not compatible with the HDPE matrix and was used merely for the purpose of comparison. HDPE was obtained from Formosa Plastics Co. (Taiwan) under the trade name Taisox 9003. The density was 0.954 g/cm^3, and the melt index (MI) was 0.3 g/10 min (2.16 kg, 190°C), as provided by the supplier. WF (Celluflex) was received from J. Rettenmainer & Sohne, GmbH (Germany). The distributions of the fiber length for the WFs ranged from 10 to 150 μm with a diameter of approximately 25 μm. The apparent density was 0.11 g/cm^3. LLDPE-*g*-MA and HDPE-*g*-MA, with the trade names MB 226D and MB 100D, were manufactured by DuPont Chemical (Wilmington, DE). PP-*g*-MAs were commercial grades from Uniroyal Crompton (Middlebury, CT) under the trade name PB3002. SEBS-*g*-MA containing 28 wt % styrene was Shell Kraton (Houston, TX) 1901X. Details of the MI and degree of grafting for these compatibilizers are listed in Table I.

Sample preparations

WF was predried at 65°C for 48 h in an air-circulated oven. The mixing of HDPE and WF with various types of compatibilizers was carried out with a corotating twin-screw extruder (Sino-Alloy, Taiwan) of type Sino PSM30 with a screw diameter of 31.2 mm and a length-to-diameter ratio of 45. The screw speed was maintained at 80 rpm, and the barrel temperatures

TABLE I
Physical Properties of Compatibilizers

Compatibilizer	Matrix				
	HDPE9003	LLDPE-*g*-MA	HDPE-*g*-MA	PP-*g*-MA	SEBS-*g*-MA
MI[a] (g/10min 190°C)	0.3	0.6	0.8	2.9	17.5
Degree of grafting[b] (wt %)		0.9	0.9	0.2	2

[a] Measured by ASTM 1238.
[b] Provided by the supplier.

ranged from 170 to 200°C. The extrudate was pelletized and then oven-dried for 48 h at 70°C. Tensile and Izod impact test specimens complied with ASTM Standards D 638 and D 256, respectively, were then prepared with an injection-molding machine (Battenfeld BA 750CD plus, Battenfeld, Germany).

Measurements

All test specimens were preconditioned at 25°C and 60% humidity for 48 h before testing. Tensile measurements were conducted at a crosshead speed of 5 mm/min with an Instron Machine model 4467 (Canton, MA). The tensile strength, elongation, and modulus were recorded. Notched Izod impact testing was performed with a Custom Scientific Instruments CS-137 (Indianapolis, IN) at room temperature.

The morphology of the fractured tensile and impact test specimens at room temperature were elucidated with a scanning electron microscope (Topcon SM300, Hong Kong, China). All samples were sputtered with gold before microscopic observations.

The dynamic mechanical thermal properties of the composite damping peak [or loss tangent (tan δ)] and storage modulus (E') were measured with DMTA (PerkinElmer 7e, Norwalk, CT). The typical specimen size was 3 mm × 12 mm × 13 mm, and the data presented in this study were run at 1 Hz with a three-point bending mode with a span of 10 mm over a temperature range of −140 to 50°C at a heating rate of 2°C/min.

The treated wood composites were Soxhlet-extracted with hot xylene at 135°C for 72 h. The extracted WFs were then decanted and dried. IR absorption spectra of treated and untreated WFs were obtained with the diffuse reflectance Fourier transform (DRIFT) accessory[29,30] on a BioRad FTS-40 FTIR spectrophotometer (Richmond, CA) at a resolution of 4 cm^{-1} with 100 sample scans for each spectrum at 4000–500 cm^{-1}. Background spectra were obtained with pure, powdered potassium bromide. No dilution of the powdered wood sample in powdered KBr was required to obtain a spectrum. The samples were transferred to 4-mm-diameter cups with slight compression and then were leveled with a spatula. Diffuse reflectance spectra were plotted as the Kubelka–Munk function, which is suitable for quantitative analysis.

RESULTS AND DISCUSSION

Mechanical properties

The effects of the compatibilizer loadings on the tensile modulus of HDPE/WF composites containing various types of compatibilizers are shown in Figure 1. The modulus has been determined at a 0.5% strain on the stress–strain curve. The loading of the compatibilizer is expressed as parts per hundred parts of resin (phr) based on 70 parts of HDPE and 30 parts of WF. The tensile moduli of PP-*g*-MA- and HDPE-*g*-MA-treated composites are higher than those for other compatibilizers at all loadings. The moduli of modified composites increase with the loading of PP-*g*-MA. However, the tensile moduli of the modified composites are reduced with the addition of the other three compatibilizers. PP-*g*-MA, with PP as its backbone, is generally stiffer than PE-*g*-MAs, and PP-*g*-MA-modi-

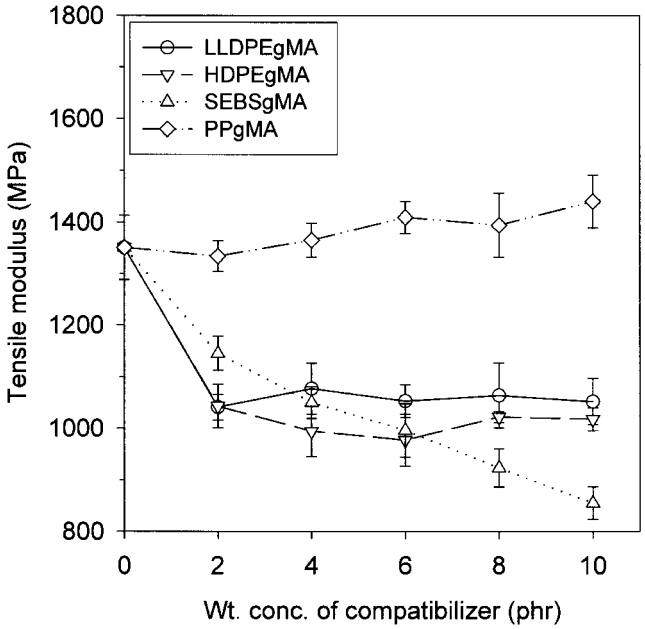

Figure 1 Tensile modulus of HDPE/WF composites with various types of compatibilizers.

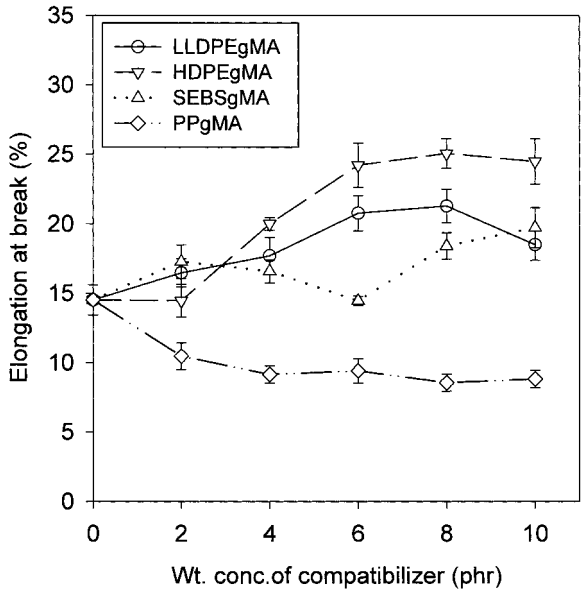

Figure 2 EB of HDPE/WF composites with various types of compatibilizers.

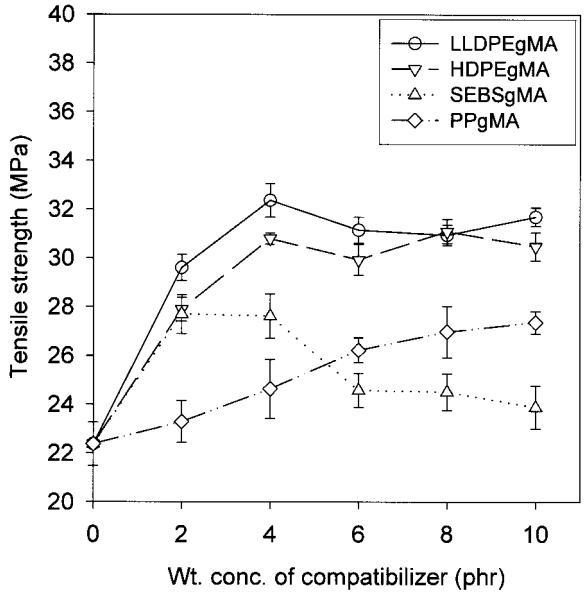

Figure 3 Tensile strength of HDPE/WF composites with various types of compatibilizers.

fied composites yield higher moduli than the other systems. The addition of SEBS-*g*-MA causes the greatest reduction in modulus, presumably because of its butylene block, which is elastomeric in nature.

Contrary to the positive effect on the tensile modulus, the addition of stiff components such as PP-*g*-MA yields composites with the elongation at break (EB) lower than that of untreated ones (see Fig. 2). However, the addition of the ductile components, that is, the rest of the compatibilizers, shows significant improvement in EB, which increases with increasing compatibilizer loading. The low EB of PP-*g*-MA-treated composites may be associated with the high stiffness of PP-*g*-MA and its poor compatibility with the HDPE matrix.

The effects of the compatibilizer loading on the tensile strength of HDPE/WF composites are shown in Figure 3. Regardless of the types of compatibilizers, a positive effect on the tensile strength for these compatibilized composites can be seen with respect to the unmodified system. This might be attributed to the enhanced interfacial interaction between HDPE and WF. In general, the tensile strength increases significantly with the addition of only small amounts of compatibilizers (2 phr) and tends to level off when the dosages are greater than 6–8 phr in all cases. Among them, compatibilized composites with PE-*g*-MA exhibit greater tensile strength than those with PP-*g*-MA. Addition to providing an improvement in the interfacial adhesion, PE-*g*-MAs are similar to the HDPE matrix in their chemical structures. Furthermore, the MIs (see Table I) of LLDPE-*g*-MA and HDPE-*g*-MA are closer to that of the HDPE matrix, which may imply a resemblance in the molecular weight or chain length among these polymers.[31] This, in turn, promotes miscibility between the PE compatibilizers and the matrix and, consequently, yields greater tensile strength. In addition, SEBS-*g*-MA-compatibilized composites show the least improvement, presumably because of its elastomeric nature, which also causes a significant drop in the modulus of the composite.

Impact strengths of compatibilized and unmodified composites are shown in Figure 4. The improvement in the impact strength of the composites with PE-*g*-MAs (LLDPE-*g*-MA and HDPE-*g*-MA) as compatibilizers is again superior to the compatibilized systems with PP-*g*-MA. The impact strength of the composites

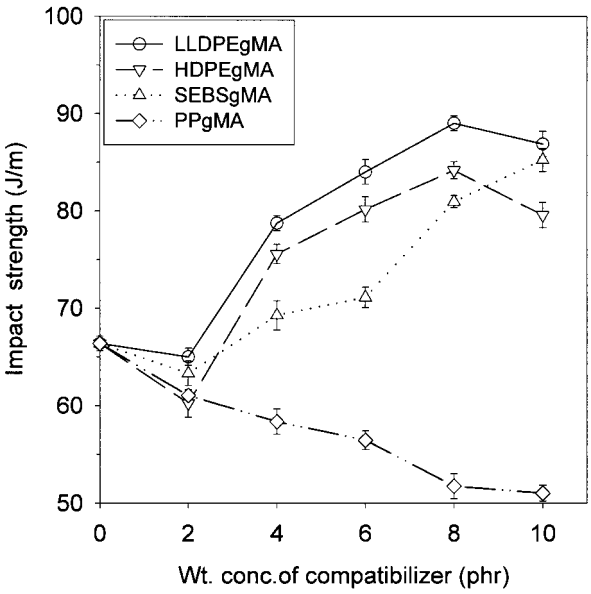

Figure 4 Impact strength of HDPE/WF composites with various types of compatibilizers.

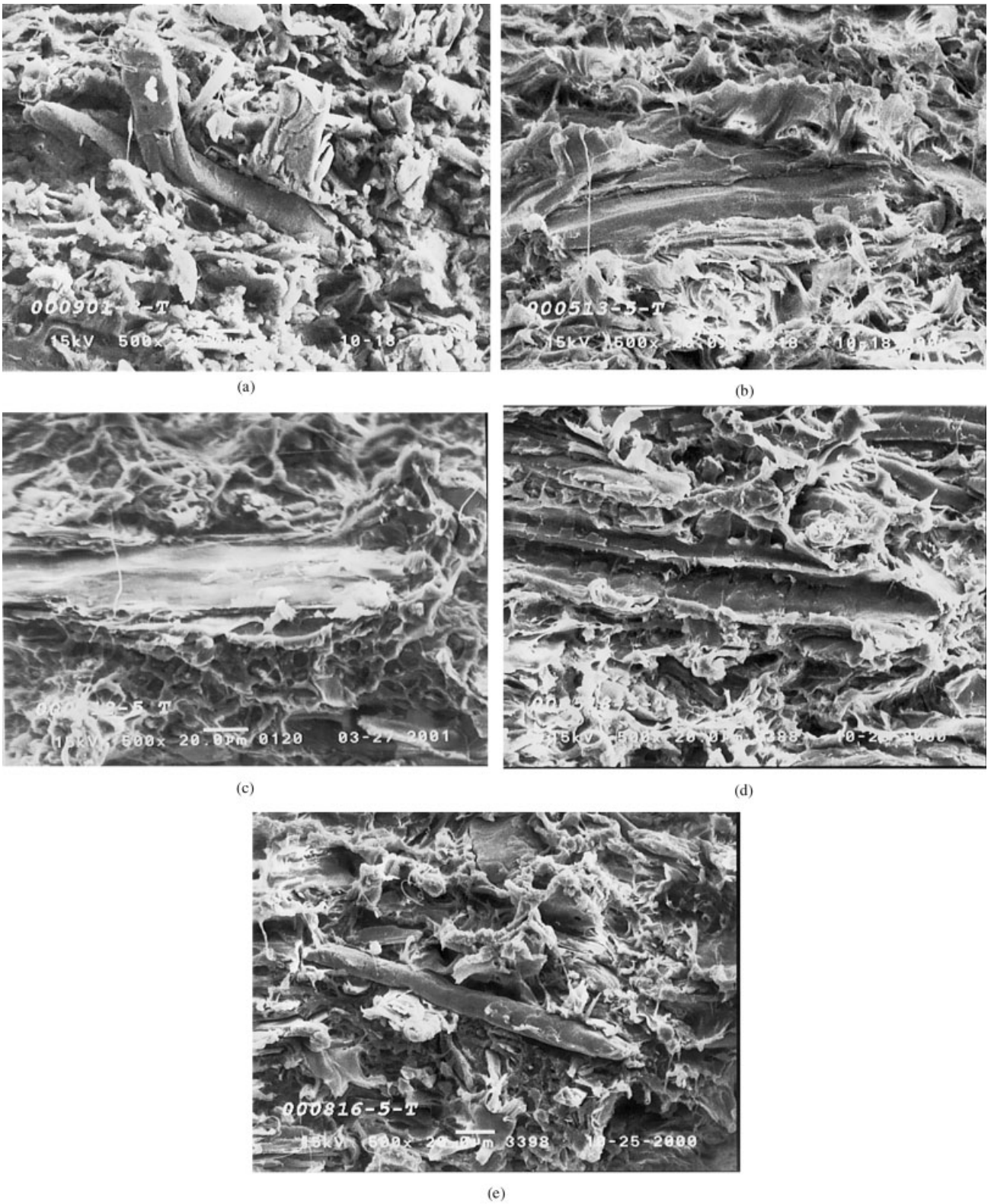

Figure 5 SEM micrographs of fracture surfaces of tensile specimens of (a) an unmodified composite, (b) an LLDPE-*g*-MA-compatibilized composite, (c) an HDPE-*g*-MA-compatibilized composite, (d) an SEBS-*g*-MA-compatibilized composite, and (e) a PP-*g*-MA-compatibilized composite.

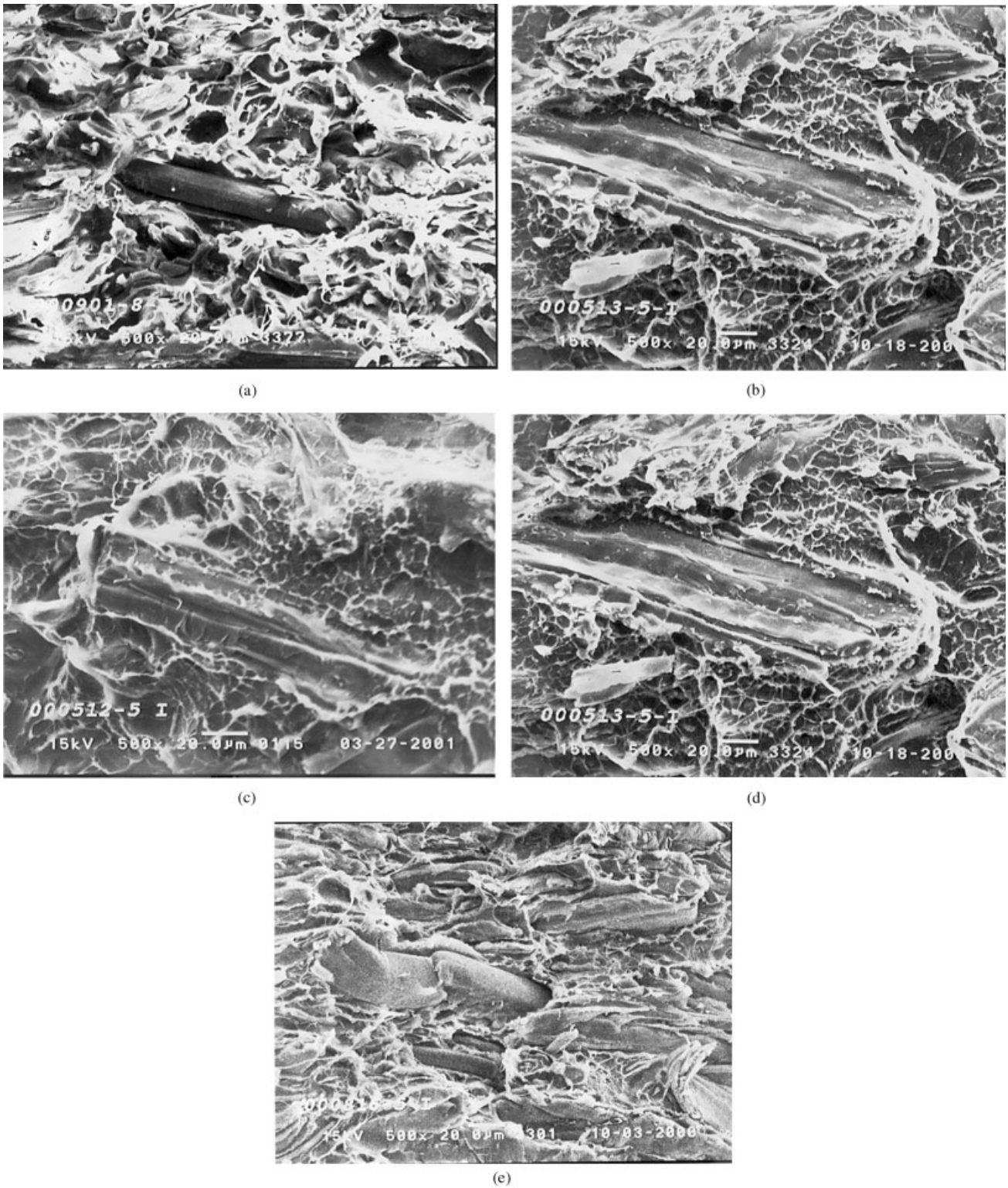

Figure 6 SEM micrographs of fracture surfaces of notched-impact specimens for (a) an unmodified composite, (b) an LLDPE-*g*-MA-compatibilized composite, (c) an HDPE-*g*-MA-compatibilized composite, (d) an SEBS-*g*-MA-compatibilized composite, and (e) a PP-*g*-MA-compatibilized composite.

increases with the loading of PE-*g*-MAs. The factors that enhance the impact strength are basically the same as those for the tensile strength. The improved interfacial adhesion and the miscibility between PE-*g*-MAs and the HDPE matrix give rise to composites of greater impact strength. Furthermore, the addition of SEBS-*g*-MA also increases the impact strength of the unmodified composite to the same level as that of

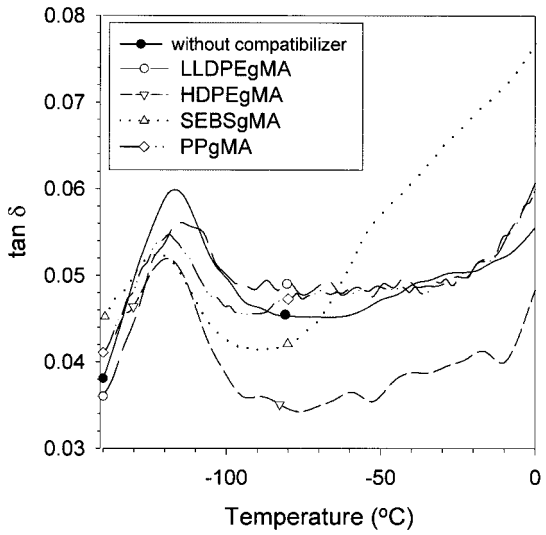

Figure 7 DMTA curves of the HDPE/WF composites at a 70/30 weight ratio with various types of compatibilizers at 10 phr. Tan δ is presented as a function of temperature.

PE-*g*-MAs. This is because the elastomeric butylene block, which is incompatible with the matrix, acts as a stress concentrator and energy absorber.[32]

However, the impact strength decreases steadily, and the loading of PP-*g*-MA increases; this is contrary to the enhancement in the tensile strength. Several possibilities might result in this difference, such as the compatibility between the compatibilizer and matrix resin and the inherent properties of the compatibilizer. The incompatibility of PP-*g*-MA with the PE matrix is well known.[4,13] In addition, the chain mobility of the compatibilizer located at the interface is associated with its glass-transition temperature. For PP with a glass transition of about −10°C, the ability to prevent brittle catastrophic crack growth in a high-speed impact test is, therefore, quite limited. However, the relatively low grafting level of maleic anhydride on PP might not be able to form enough interfacial bonding between the HDPE matrix and WF surfaces. Further discussion on the interfacial region is presented later with the fractography and DMTA analysis.

Morphology

Figure 5 shows the distinct morphology of the fracture surfaces of tensile specimens for unmodified and compatibilized composites based on the SEM observations. Besides the relatively smooth surface observed on the WF filler, there are finite gaps near the interfacial region between the PE matrix and WF indicating poor adhesion for an unmodified composite. However, no clear gap is seen in the rough interfacial region between the PE matrix and WF for individual compatibilized systems. In addition, there does not seem to be a very significant difference at the interface when a comparison is made of the composites with all four compatibilizers. This provides qualitative evidence for the existence of adhesive bonds between the surfaces. According to this SEM study, all the compatibilizers used in the HDPE/WF composite improve the interfacial interaction in the interface, and this results in an enhancement in the tensile strength.

SEM observations of the fracture surfaces of notched-impact specimens for unmodified and compatibilized systems are shown in Figure 6. As indicated earlier, poor adhesion is found between the PE matrix and wood filler for an unmodified composite. For compatibilized systems, one would expect behavior at the interface similar to that seen in the fracture surfaces of tensile specimens. However, there is an exception when PP-*g*-MA is used as a compatibilizer. The interfacial region appears to resemble that of an unmodified system, suggesting the formation of a weak interphase between the HDPE and wood filler. This peculiar observation of the SEM micrographs between tensile and impact specimens for the PP-*g*-MA-compatibilized composite might lie in the incompatibility of the PP backbone with the HDPE matrix. Additionally, the limited mobility of the molecular chain motion of PP, which is manifested in a high-speed impact test compared with a low-speed tensile measurement, would lead to less of a chance for further promoting the shear yielding of the PE matrix to stop the crack growth. These examinations confirm the low impact strength of the PP-*g*-MA-compatibilized composite shown in Figure 4.

Dynamic mechanical thermal measurements

For simplicity, the results of the DMTA analysis shown in Figure 7 are exemplified by the tan δ data for

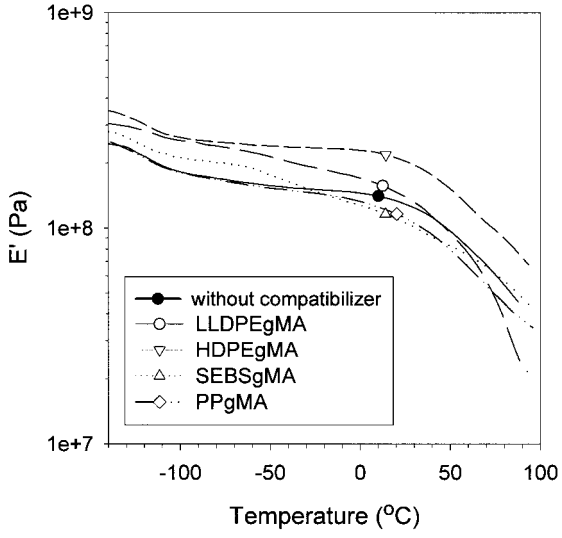

Figure 8 DMTA curves of the HDPE/WF composites at a 70/30 weight ratio with various types of compatibilizers at 10 phr. *E′* is presented as a function of temperature.

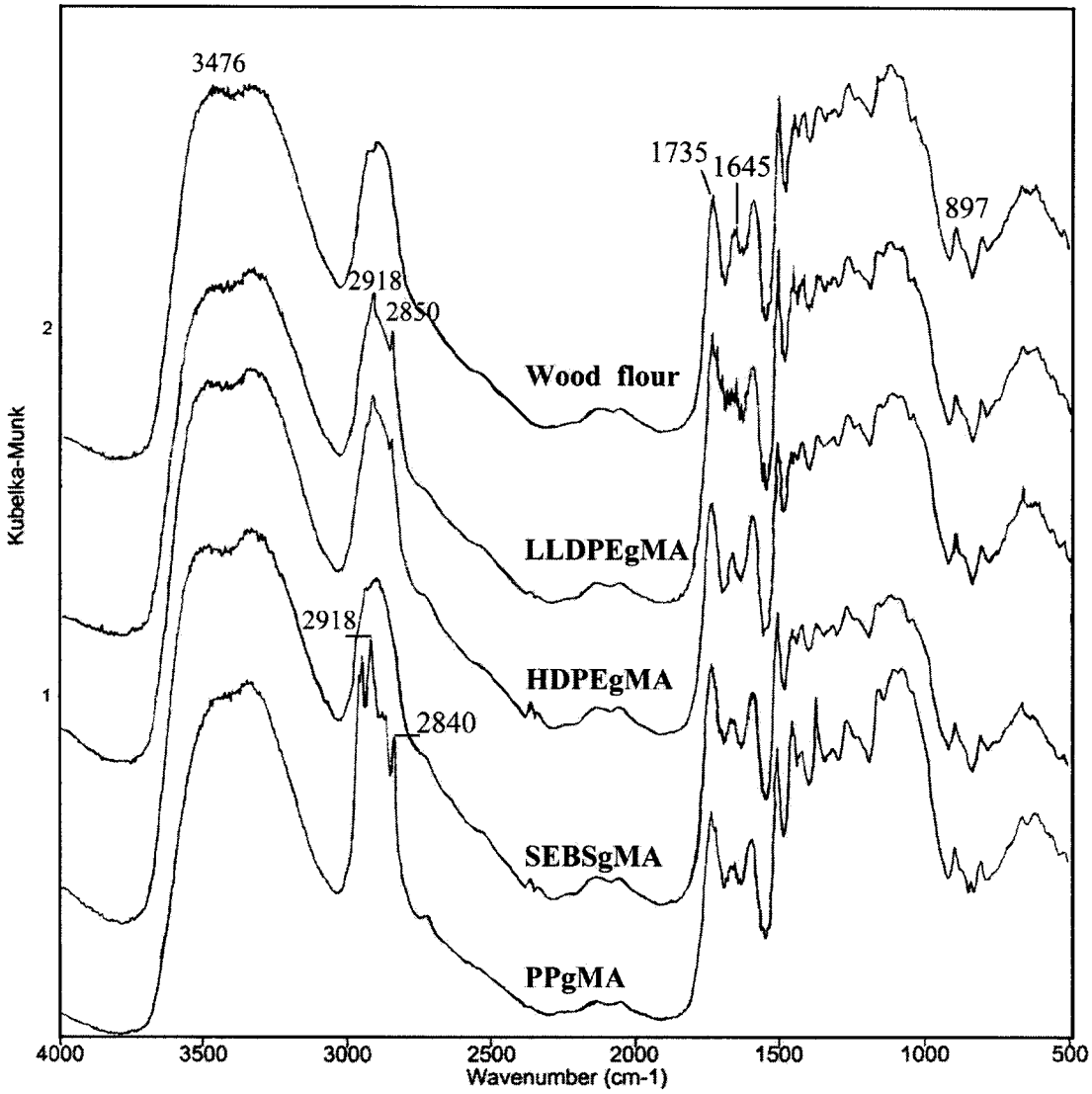

Figure 9 DRIFT spectra of untreated WF and treated flour with various types of compatibilizers at 10 phr.

HDPE/WF composites without compatibilizers and with various compatibilizers at 10 phr. In the systems studied, there is one major transition, that is, the HDPE γ transition, which occurs at about -115°C. The measurement can give knowledge about the interfacial behavior of composites. Tan δ broadens and the peak position shifts if there is an interaction between the matrix polymer and the filler/reinforcement.[33] Evidently, both the apparent glass-transition temperature and the amplitude of the tan δ peak respond to the nature of the polymer/filler interface. As can be seen in Figure 7, the peak amplitude decreases with the addition of compatibilizers. This is expected because the decrease in amplitude indicates that the number of mobile segments involved has decreased on account of improved adhesion between the filler and matrix. Furthermore, the tan δ peak position of LLDPE-*g*-MA-modified systems is shifted a little toward a higher temperature. The shift in the tan δ peak also shows that the molecular motion is restricted, and this confirms the strong interaction between the filler and matrix due to better compatibility between the LLDPE-*g*-MA and HDPE matrix.

Figure 8 shows E' as a function of temperature for the same systems. Besides a decrease in tan δ, it is well known that the use of the filler increases E' and that the increase is usually greatest in the transition and plateau regions of the viscoelastic spectrum.[33] The addition of compatibilizers has increased E' of the composites at the transition and plateau regions, except for the PP-*g*-MA-modified system, which does not show much of a difference from the untreated system. The increase in E' also indicates enhanced adhesion between the filler and matrix, leading to an interphase of higher stiffness than that of an untreated system.

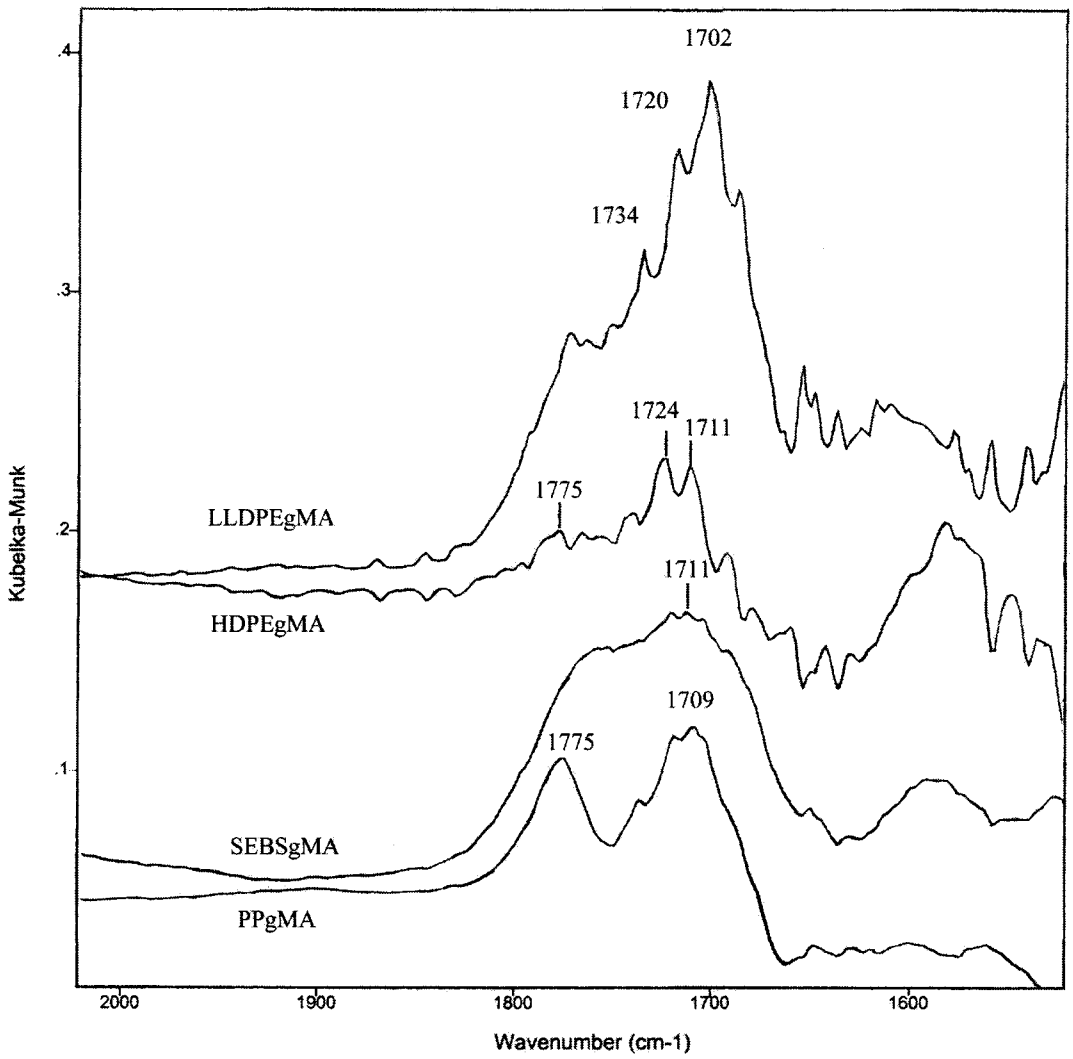

Figure 10 C═O stretching absorption peaks from normalized DRIFT difference spectra of compatibilized composites.

IR spectroscopy

The IR spectra of the DRIFT analysis for untreated and extracted WFs coated with different compatibilizers are shown in Figure 9. The major FTIR absorption bands and assignments of absorption bands for untreated WFs of a lignocellulosic nature are shown later. The absorption bands at 3500–3100 cm^{-1} for WFs are characteristic of various hydrogen-bonded hydroxyl (OH) stretching vibrations. Next to the hydroxyl bands, there are absorption bands at 3100–2600 cm^{-1} due to the CH stretching vibration of CH_2 and CH_3 groups. The peaks at 1735 and 1645 cm^{-1} are the characteristic peaks for carbonyl (C═O) stretching, which is due to the presence of ester groups in WFs.[30] The strong peak at 897 cm^{-1} is due to the stretching vibration of the glucose ring.

For coated WFs, the disappearance of the hydroxyl peak at 3476 cm^{-1} can clearly be seen, indicating the esterification reaction. Moreover, an apparent increase in the peak intensity of the CH absorption bands at 2918 cm^{-1} can also be detected in the spectra of all coated WFs. However, the most important features of the spectra are the carbonyl absorption occurring in the 1750–1720-cm^{-1} region, arising from the ester bond between the wood and the anhydride or acid moiety. Furthermore, because uncoated WFs already have ester groups that absorb at 1735 cm^{-1}, the confirmation of esterification between WFs and maleated polyolefins may only be indicated by an increase in the intensity of the absorption bands near this peak. Figure 10 shows the normalized DRIFT difference spectrum of coated WFs with different compatibilizers. The absorption peaks were normalized at 897 cm^{-1} to an arbitrary value. The presence of strong and sharp absorption bands can be seen at 1711–1702 cm^{-1}, and these may possibly be due to the carbonyl stretching of carboxyl groups in maleated polyolefins, whereas the absorption bands at 1775 cm^{-1} may be

due to anhydride carbonyl symmetrical and unsymmetrical stretching vibrations. However, the difference spectra do not indicate the presence of any distinct absorption bands near 1730 cm^{-1}, except for LLDPE-*g*-MA- and HDPE-*g*-MA-modified system. Although the absorption peaks at 1734 and 1720 cm^{-1} for LLDPE-*g*-MA and at 1724 cm^{-1} for HDPE-*g*-MA are not very well-defined, they may be associated with the ester links between hydroxyl groups of WFs and the anhydride or acid groups of polyolefinic compatibilizers.[30]

CONCLUSIONS

The effects of various types of compatibilizers, including LLDPE-*g*-MA, HDPE-*g*-MA, SEBS-*g*-MA, and PP-*g*-MA, on the mechanical properties of HDPE/WF composites have been investigated in this study. LLDPE-*g*-MA provides the greatest enhancement in the tensile strength and impact resistance. Presumably, there is good compatibility between the HDPE matrix and the compatibilizer because of the similarity of the chain structures of both resins. In addition, strong interfacial bonding resulting from the chemical reaction between maleic anhydride on the compatibilizer and the hydroxyl groups of WF further supports the improved mechanical properties. These are clearly revealed through an SEM analysis. Although HDPE-*g*-MA has the same degree of grafting as LLDPE-*g*-MA, the composites modified by LLDPE-*g*-MA give slightly better mechanical properties than HDPE-*g*-MA. LLDPE-*g*-MA may be more compatible with the HDPE matrix because its MI is more similar to that of the matrix than HDPE-*g*-MA.

Similar behaviors are observed through SEM micrographs for the SEBS-*g*-MA-compatibilized system. Although the high degree of grafting enhances the adhesion between the wood filler and matrix, the improvement in the impact strength is mainly due to the elastomeric block, which is incompatible with the matrix. However, the ductile nature of the elastomeric block causes the least improvement in tensile strength among the compatibilizers under consideration.

Finally, when a close examination is focused on the interface between the PE and wood filler compatibilized with PP-*g*-MA, two different kinds of debonding morphology are found in tensile and impact fracture specimens. The tensile fracture surface exhibits a rough interface on the wood filler, and this suggests that debonding may occur at the ductile phase of the HDPE matrix. The impact fracture surface exhibits a smooth interface, and this indicates poor adhesion between the wood filler and matrix; therefore, debonding may occur right on the surface of the wood filler. These observations lead to improved tensile strength but a loss in the impact strength of the composite.

References

1. Zavin, E. Adv Chem Ser 1984, 207, 349.
2. Zadorecki, P.; Michell, A. J. Polym Compos 1989, 10, 69.
3. Maldas, D.; Kokta, B. V. Compos Interfaces 1993, 1, 87.
4. Gauthier, R.; Joly, C.; Coupas, A. C.; Gauthier, H.; Escoubes, M. Polym Compos 1998, 19, 287.
5. Benedetto, A. T. D.; Haddad, G.; Schilling, C.; Osterholtz, F. In Interfacial Phenomena in Composite Materials; Jones, F. R., Ed.; Butterworth–Heinemann: Boston, MA, 1989.
6. Cousin, P.; Bataille, P.; Schreiber, H. P.; Sapieha, S. J Appl Polym Sci 1989, 37, 3057.
7. Raj, R. G.; Kokta, B. V.; Deinbela, C.; Sanschagrain, B. J Appl Polym Sci 1989, 38, 1987.
8. Raj, R. G.; Kokta, B. V.; Daneault, C. J Mater Sci 1990, 25, 1851.
9. Maldas, D.; Kokta, B. V. Polym J 1991, 10, 1163.
10. Freischmidt, G.; Michell, A. J. Polym Int 1991, 24, 241.
11. Nogellova, Z.; Kokta, B. V.; Chodak, I. J Macromol Sci Pure Appl Chem 1998, 35, 1069.
12. Klason, C.; Kubat, J.; Stromvall, H. E. Int J Polym Mater 1984, 10, 159.
13. Woodhams, R. T.; Thomas, G.; Rodgers, D. K. Polym Eng Sci 1984, 24, 1166.
14. Dalvag, H.; Klason, C.; Stromvall, H. E. Int J Polym Mater 1985, 11, 9.
15. Kishi, H.; Yoshioka, M.; Yamanoi, A.; Shiraishi, N. Mokuzai Gakkaishoi 1988, 34, 133.
16. Han, G.-S.; Ichinose, H.; Takase, S.; Shiraishi, N. Mokuzai Gakkaishoi 1989, 35, 1100.
17. Takase, S.; Shiraishi, N. J Appl Polym Sci 1989, 37, 645.
18. Raj, R. G.; Kokta, B. V.; Daneault, C. Int J Polym Mater 1989, 12, 239.
19. Maldas, D.; Kokta, B. V. J Appl Polym Sci 1990, 40, 917.
20. Felix, J. M.; Gatenholm, P. J Appl Polym Sci 1991, 42, 609.
21. Myers, G. E.; Chahyadi, I. S.; Coberly, C. A.; Ermer, D. S. Int J Polym Mater 1991, 15, 21.
22. Raj, R. G.; Kokta, B. V. Polym Eng Sci 1991, 31, 1358.
23. Oksman, K. Wood Sci Technol 1996, 30, 197.
24. Oksman, K.; Lindberg, H. Holzforschung 1998, 52, 661.
25. Oksman, K.; Lindberg, H.; Holmgren, A. J Appl Polym Sci 1998, 69, 201.
26. Scott, C.; Ishida, H.; Maurer, F. H. J. J Mater Sci 1987, 22, 3963.
27. Hindryckx, F.; Dubois, P.; Patin, M.; Jerome, R.; Teyssie, P.; Garcia Marti, M. J Appl Polym Sci 1995, 56, 1093.
28. Wang, Y.; Chan, H.-C.; Lai, S.-M.; Shen, H.-F. Int Polym Process 2001, 16, 100.
29. Fuller, M. P.; Griffiths, P. R. Anal Chem 1978, 50, 1906.
30. Kazayawoko, M.; Balatinecz, J. J.; Woodhams, R. T. J Appl Polym Sci 1997, 66, 1163.
31. Brydson, J. A. Plastics Materials, 6th ed.; Butterworth-Heinemann: Oxford, 1995; p 211.
32. Utracki, L. A.; Khanh, T. V. In Multicomponent Polymer Systems; Miles, I. S.; Rostami, S., Eds.; Polymer Science and Technology Series; Longman Scientific: London, 1992.
33. Nielsen, L. E. Mechanical Properties of Polymers and Composites; Marcel Dekker: New York, 1974; Vol. 2.